



OPEN

Cytokine release syndrome in a patient with colorectal cancer after vaccination with BNT162b2

Lewis Au^{1,2,15}, Annika Fendler^{1,15}, Scott T. C. Shepherd^{1,2}, Karolina Rzeniewicz¹, Maddalena Cerrone^{3,4}, Fiona Byrne¹, Eleanor Carlyle², Kim Edmonds², Lyra Del Rosario², John Shon⁵, Winston A. Haynes⁵, Barry Ward¹, Ben Shum^{1,2}, William Gordon¹, Camille L. Gerard^{1,6}, Wenyi Xie¹, Nalinie Joharatnam-Hogan², Kate Young², Lisa Pickering², Andrew J. S. Furness², James Larkin², Ruth Harvey⁷, George Kassiotis⁸, Sonia Gandhi^{9,10}, Crick COVID-19 Consortium*, Charles Swanton¹¹, Charlotte Fribbens^{12,13}, Katalin A. Wilkinson³, Robert J. Wilkinson^{3,4}, David K. Lau¹³, Susana Banerjee¹⁴, Naureen Starling¹³, Ian Chau¹³, CAPTURE Consortium* and Samra Turajlic^{1,2}✉

Patients with cancer are currently prioritized in coronavirus disease 2019 (COVID-19) vaccination programs globally, which includes administration of mRNA vaccines. Cytokine release syndrome (CRS) has not been reported with mRNA vaccines and is an extremely rare immune-related adverse event of immune checkpoint inhibitors. We present a case of CRS that occurred 5 d after vaccination with BNT162b2 (tozinameran)—the Pfizer-BioNTech mRNA COVID-19 vaccine—in a patient with colorectal cancer on long-standing anti-PD-1 monotherapy. The CRS was evidenced by raised inflammatory markers, thrombocytopenia, elevated cytokine levels (IFN- γ /IL-2R/IL-18/IL-16/IL-10) and steroid responsiveness. The close temporal association of vaccination and diagnosis of CRS in this case suggests that CRS was a vaccine-related adverse event; with anti-PD1 blockade as a potential contributor. Overall, further prospective pharmacovigilance data are needed in patients with cancer, but the benefit-risk profile remains strongly in favor of COVID-19 vaccination in this population.

CRS/cytokine storm is a systemic inflammatory response, characterized by excessive cytokine release (that is, elevated INF- γ , IL-6, IL-10 and IL-2R)¹. CRS might develop after infection (including COVID-19) or due to iatrogenic causes, most notably chimeric antigen receptor T cell (CAR-T) therapy and, less frequently, cytotoxic chemotherapy or stem cell transplantation^{1–3}. Extremely rarely, it occurs after immune checkpoint inhibitor (ICI) therapy^{1,4}, and, to our knowledge, it has not been reported after administration of any vaccine. Here we report a case of CRS after vaccination with BNT162b2 (tozinameran), an mRNA COVID-19 vaccine.

A 58-year-old male commenced anti-PD-1 monotherapy (an investigational ICI within an ongoing interventional clinical trial;

NCT02715284) in February 2019 for the treatment of mismatch repair-deficient colorectal cancer (MMRd CRC) metastatic to mesentery and rectus muscle (Fig. 1a). Two months after treatment initiation, he experienced a neurological immune-related adverse event (irAE) with worsening ataxia (grade 1 to grade 2, and magnetic resonance imaging changes in pons, medulla and cerebellum) on the background of pre-existing spinocerebellar ataxia of unknown etiology. ICI was suspended, and he was commenced on 1 mg kg⁻¹ prednisolone (tapered over 1 month), and ataxia returned to grade 1 (baseline). Anti-PD-1 therapy was re-started in June 2019 (Fig. 1a), with stable disease as per immune-related Response Evaluation Criteria in Solid Tumors. In March 2020 (13 months after commencing ICI), he developed an endocrine irAE (grade 1 hypocortisolemia from adrenocorticotrophic hormone deficiency; Fig. 1a) and was commenced on physiological corticosteroid replacement (prednisolone, 3 mg daily). Disease control was maintained, and the last ICI dose was administered in December 2020, 27 d before BNT162b2.

The patient had no history of severe acute respiratory syndrome coronavirus 2 (SARS-CoV-2) infection and had negative SARS-CoV-2 serological tests in June and October 2020. He received the first dose of BNT162b2 vaccine on 29 December 2020 (Fig. 1a) without immediate adverse events, except for grade 1 inflammation at the vaccination site. Five days later (32 d after the last anti-PD-1 dose), he presented with myalgia, 2-d history of diarrhea (grade 1) and 1-d history of fever (38.4°C) despite anti-pyretics (ibuprofen) use. On admission to the hospital, his vital signs were as follows: oxygen saturation, 100% on room air; respiratory rate, 18 breaths per minute; blood pressure, 111/71 mmHg; heart rate, 86 beats per minute; and temperature, 36.7°C. Laboratory investigations revealed elevated inflammatory markers (C-reactive protein (CRP)),

¹Cancer Dynamics Laboratory, The Francis Crick Institute, London, UK. ²Skin and Renal Units, The Royal Marsden NHS Foundation Trust, London, UK.

³Tuberculosis Laboratory, The Francis Crick Institute, London, UK. ⁴Department of Infectious Disease, Imperial College London, London, UK. ⁵Serimmune, Inc., Goleta, CA, USA. ⁶Precision Oncology Center, Lausanne University Hospital (CHUV), Lausanne, Switzerland. ⁷Worldwide Influenza Centre, The Francis Crick Institute, London, UK. ⁸Retroviral Immunology Laboratory, The Francis Crick Institute, London, UK. ⁹Neurodegeneration Biology Laboratory, The Francis Crick Institute, London, UK. ¹⁰UCL Queen Square Institute of Neurology, Queen Square, London, UK. ¹¹Cancer Evolution and Genome Instability Laboratory, The Francis Crick Institute, London, UK. ¹²Acute Oncology Service, The Royal Marsden NHS Foundation Trust, London, UK. ¹³Gastrointestinal and Lymphoma Unit, The Royal Marsden NHS Foundation Trust, Sutton, UK. ¹⁴Gynaecology Unit, The Royal Marsden NHS Foundation Trust and Institute of Cancer Research, London, UK. ¹⁵These authors contributed equally: Lewis Au, Annika Fendler. *Lists of authors appear at the end of the paper.

✉e-mail: samra.turajlic@crick.ac.uk

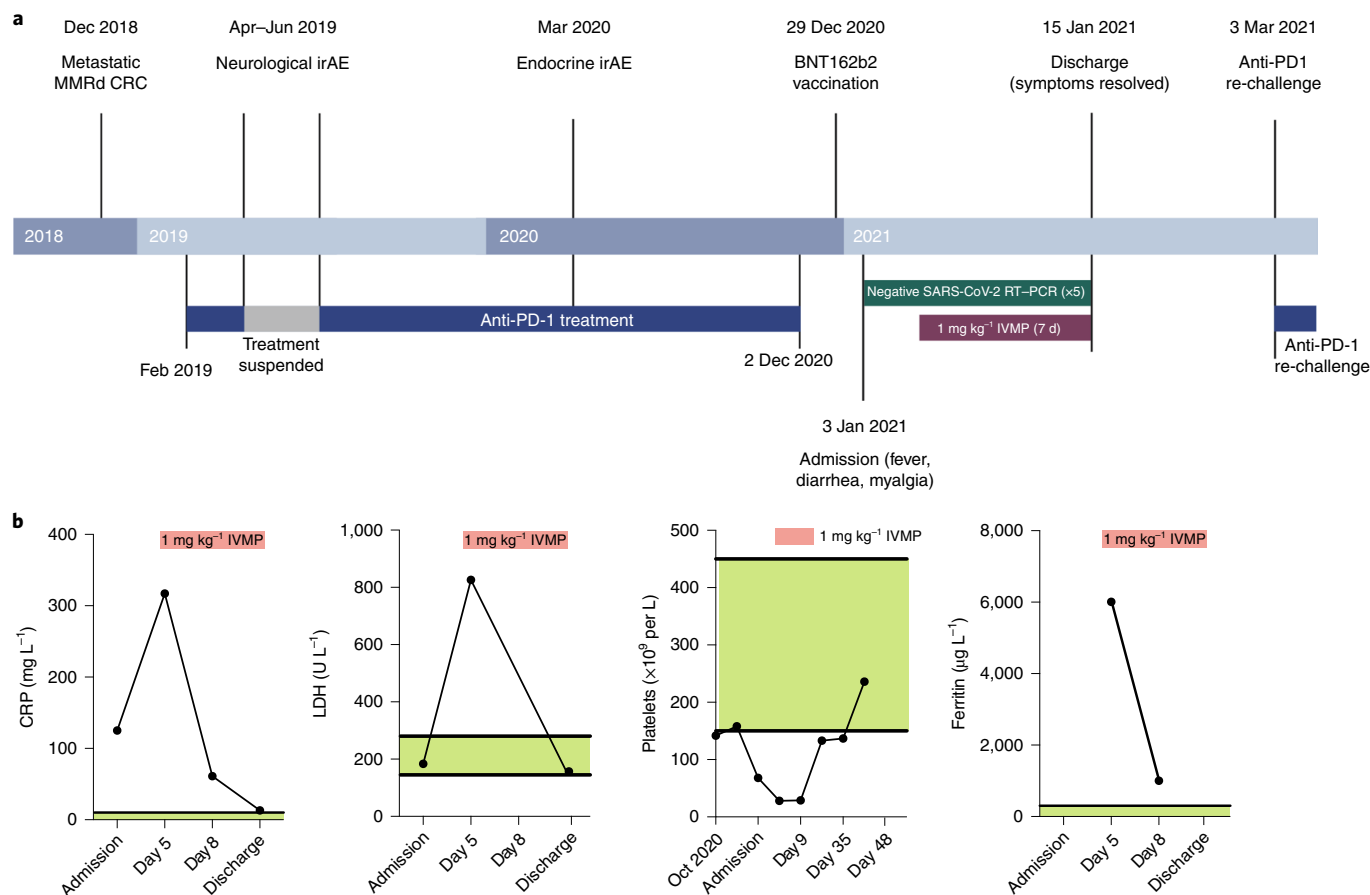


Fig. 1 | Clinical course from cancer diagnosis and inflammatory markers during CRS. a, Clinical timeline from diagnosis of metastatic MMRd CRC to CRS after one dose of BNT162b2 vaccine. Created with BioRender.com. **b**, CRP, LDH, platelet count and ferritin levels during the course of admission. Normal ranges are indicated in green. Treatment with IVMP is indicated in red.

125 mg L⁻¹ (normal, <6 mg L⁻¹); serum lactate dehydrogenase (LDH), 184 U L⁻¹ (normal range, 120–246 U L⁻¹); and thrombocytopenia (68 × 10⁹ cells per liter (normal range, 150–410 cells per liter)), confirmed on microscopy (Fig. 1b). Empirical treatment with broad-spectrum intravenous antibiotics was commenced; however, blood and urine cultures were negative, as was SARS-CoV-2 RT-PCR of serial nasopharyngeal swabs (Fig. 1a). There were no clinical signs or symptoms during admission or follow-up to suspect a thrombotic event in this patient. Computed tomography of thorax, abdomen and pelvis revealed no nidus of infection or thrombosis and showed stable disease with respect to cancer. The patient was not heparinized. Over the next 5 d, fevers up to 39.8 °C continued, with worsening thrombocytopenia (28 × 10⁹ cells per liter) and increasing inflammatory markers (CRP, 317 mg L⁻¹; LDH, 849 U L⁻¹), including significantly elevated ferritin (6,010 µg L⁻¹ (normal range, 18–464 µg L⁻¹)) (Fig. 1b). At this point (5 d after admission), CRS was suspected (grade 3), and he was commenced on 1 mg kg⁻¹ of intravenous methylprednisolone (IVMP), and antibiotics were ceased 3 d later. Biochemical and hematological indices normalized within 7 d of IVMP initiation (Fig. 1b), and the patient was afebrile and asymptomatic upon discharge home with a weaning corticosteroid regimen. He remained well and was re-challenged with anti-PD-1 on 8 February 2021 (36 d after initial presentation) without any adverse events (Fig. 1a). He did not receive the second dose of BNT162b2.

To explore the features of his presentation further, we performed longitudinal cytokine analysis, before and after IVMP. An exaggerated type 1 helper T cell (Th1) response is a frequent feature of CRS¹,

and the initial profile (day 3 of admission; Fig. 2a) indicated activation of Th1 cells (elevated MIG, IL-2R, IL-16, IFN-γ and IL-18) and macrophages (elevated MCP-1, MIP, IL-8, IL-18 and MIG). IL-10 inhibits pro-inflammatory cytokines, limiting exuberant inflammatory responses², and, although we observed elevated IL-10 on days 3–8 of admission, it evidently failed to suppress hyperinflammation in this case. Most cytokines decreased substantially during IVMP treatment, but persistent elevation of IL-2R, IL-2, IL-16 and IL-18 on day 12 of admission (Fig. 2a) indicated sustained T cell activation.

S1-reactive and neutralizing antibodies were detectable 7 d after vaccination (Fig. 2b), and the titers continued to rise during IVMP treatment, suggesting a robust vaccine-induced immune response. However, S-specific CD4⁺ and CD8⁺ T cells were undetectable on days 17 and 40 after vaccination, and no IFN-γ-producing T cells were detected (Fig. 2c,d,e and Extended Data Fig. 1a,b), consistent with reports in patients without cancer after the first dose of BNT162b2 (ref. ⁵). Data on the effect of steroids on mRNA vaccine-induced antigen-specific T cell response are limited. One study demonstrated that dexamethasone given before, but not after, an mRNA-based cancer vaccine resulted in reduced activation of antigen-specific T cells⁶. In the case under study, steroids were administered 10 d after vaccination and unlikely to have affected vaccine-specific immune response.

To identify antibody-binding epitopes, we performed a serum epitope repertoire analysis (SERA) and a protein-based immunome-wide association study (PIWAS), using a bacterial display system coupled with next-generation sequencing.

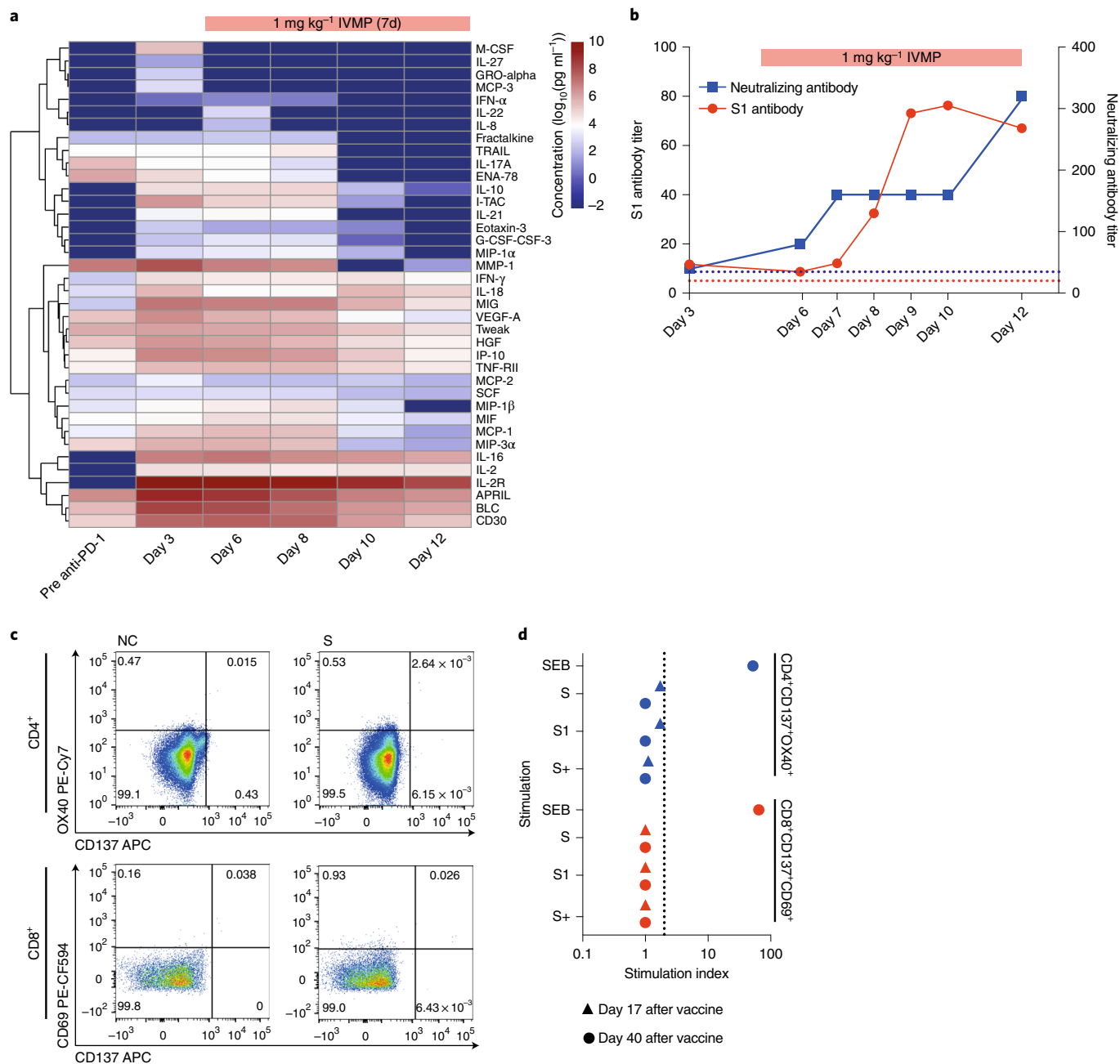


Fig. 2 | Cytokine profile and immune response to BNT162b2 vaccine. **a**, Cyto/chemokine levels were measured using the human immune monitoring 65-plex ProcartaPlex immunoassay in consecutive plasma samples. Samples were measured in duplicates. Data are presented as the \log_{10} of the concentration in pg ml^{-1} . **b**, Kinetics of S1-reactive and neutralizing antibody responses after BNT162b2. Data are presented as the reciprocal dilution of the last detected sample. IVMP treatment is indicated in red. **c**, SARS-CoV-2-specific CD4⁺ and CD8⁺ T cell response in exemplary samples after stimulation of PBMCs with spike (S) peptide pool. **d**, PBMCs were stimulated with S, S1 and S+ peptide pools representing the full length of the spike protein. SEB was used as a positive control. Data are presented as a stimulation index indicating the ratio of the frequency of CD4⁺CD137⁺OX40⁺ or CD8⁺CD137⁺CD69⁺ T cells in the sample and the negative control. SEB, Staphylococcal enterotoxin B.

The post-vaccine profile was similar to that of healthcare workers after COVID-19 mRNA vaccine, with a rise in positive signal against spike but not non-spike proteins (versus patients positive for SARS-CoV-2)⁷ (Extended Data Fig. 2a,b). This was consistent with the lack of prior SARS-CoV-2 infection as a potential contributor to the clinical presentation.

Isolated thrombocytopenia (without thrombosis) has been described with mRNA-based COVID-19 vaccines, including BNT162b2 (ref. ⁸). Given recent reports of a pathogenic platelet

factor-4 (PF4)-dependent syndrome leading to thrombotic thrombocytopenia after vaccination with ChAdOx1 nCov-19 (AstraZeneca)⁹⁻¹¹, which is a viral vector-based COVID-19 vaccine, we evaluated for PF4 antibodies, which were not detectable (Extended Data Fig. 3). Although this result does not comprehensively exclude an independent mechanism for the observed thrombocytopenia, the constellation of clinical and laboratory findings make thrombocytopenia likely to be a component of CRS in this case.

The laboratory findings in CRS are variable and relate to the underlying cause, although CRP elevation is characteristic and correlates with severity¹. Elevated ferritin and thrombocytopenia are also common abnormalities¹. Although there are no defined cytokine profiles that confirm CRS, raised IFN- γ , IL-2R, IL-18, IL-6 and IL-10 are considered key in establishing the diagnosis^{1,2}. All except IL-6 were elevated in this case. Although transient cytokine elevation (IFN- α , IFN- γ , IL-6, IFN-inducible protein-10 and IL-12p70) was observed after mRNA cancer vaccines co-administered with ICI in patients with melanoma¹², they manifest as self-limiting mild flu-like symptoms.

Fewer than 0.01% of irAEs reported in the context of anti-PD-1 monotherapy involve CRS⁴, and, to date, no CRS events have been reported after either BNT162b2 or the mRNA-1273 vaccine (Moderna)—the two mRNA-based COVID-19 vaccines currently available. ICI-related CRS typically develops a median of 4 weeks after ICI initiation (range, 1–18 weeks)⁴, making ICI as the sole cause of CRS unlikely in this patient, who commenced anti-PD1 treatment 22 months prior. The close temporal association of vaccination and clinical presentation favors the vaccine as the potential trigger of CRS in this case.

Receptor occupancy associated with anti-PD-1 agents is 2–3 months¹³, and it remains possible that CRS was triggered by the vaccine on a background of immune activation secondary to PD1 blockade that results in T cell proliferation and increased effector function¹⁴. We did not detect S-reactive T cells in the periphery, and a direct mechanism for T cells driving CRS in this case could not be demonstrated. However, vaccine-activated T cells that contributed to CRS could be resident within tissue or lymph nodes and, therefore, undetectable in the blood¹⁵. T cell cross-reactivity, as a result of sequence similarity between spike protein and tumor neoantigens, is an alternative, although less likely, cause of CRS in this case. Cross-reactivity to cardiac tissue was reported as a mechanism of ICI-related myocarditis¹⁶, and this patient's history of irAEs and the high neoantigen load (typical of MMRd CRC)¹⁷ could, in theory, increase the likelihood of T cell cross-reactivity¹⁸.

Given that patients with cancer were excluded from SARS-CoV-2 vaccine studies and are currently prioritized in COVID-19 vaccination programs globally, this case motivates prospective pharmacovigilance regarding the safety profile of COVID-19 vaccines in patients with cancer. So far, prospective data have not demonstrated additional safety concerns of BNT162b2 administration either in patients with cancer generally ($n=151$)¹⁹ or, specifically, in those who have been treated with ICI ($n=170$)²⁰. Current empirical recommendations regarding the timing of COVID-19 vaccination suggest administering 'on availability' in patients with cancer on systemic anti-cancer treatments, including ICI, cytotoxic chemotherapy and hormone therapy, and avoiding vaccination within 48–72 h of investigational products to minimize misattribution of adverse event causation²¹. Overall, as CRS in this case is an isolated report, and patients with cancer are generally more vulnerable to COVID-19 (refs. 22,23), the benefit–risk profile for COVID-19 vaccination remains strongly in favor of vaccination in this population. It is of critical importance that patients with cancer remain prioritized during vaccine rollout²⁴.

Online content

Any methods, additional references, Nature Research reporting summaries, source data, extended data, supplementary information, acknowledgements, peer review information; details of author contributions and competing interests; and statements of data and code availability are available at <https://doi.org/10.1038/s41591-021-01387-6>.

Received: 23 March 2021; Accepted: 7 May 2021;
Published online: 26 May 2021

References

- Fajgenbaum, D. C. & June, C. H. Cytokine storm. *N. Engl. J. Med.* **383**, 2255–2273 (2020).
- Shimabukuro-Vornhagen, A. et al. Cytokine release syndrome. *J. Immunother. Cancer* **6**, 56 (2018).
- Neelapu, S. S. et al. Chimeric antigen receptor T-cell therapy - assessment and management of toxicities. *Nat. Rev. Clin. Oncol.* **15**, 47–62 (2018).
- Ceschi, A. et al. Immune checkpoint inhibitor-related cytokine release syndrome: analysis of WHO Global Pharmacovigilance Database. *Front. Pharmacol.* **11**, 557 (2020).
- Prendecki, M. et al. Effect of previous SARS-CoV-2 infection on humoral and T-cell responses to single-dose BNT162b2 vaccine. *Lancet* **397**, 1178–1181 (2021).
- Vormehr, M. et al. Dexamethasone premedication suppresses vaccine-induced immune responses against cancer. *Oncimmunology* **9**, 1758004 (2020).
- Haynes, W. A. et al. High-resolution mapping and characterization of epitopes in COVID-19 patients. Preprint at <https://www.medrxiv.org/content/10.1101/2020.11.23.20235002v1.full> (2020).
- Lee, E.-J. et al. Thrombocytopenia following Pfizer and Moderna SARS-CoV-2 vaccination. *Am. J. Hematol.* **96**, 534–537 (2021).
- Scully, M. et al. Pathologic antibodies to platelet factor 4 after ChAdOx1 nCoV-19 vaccination. *N. Engl. J. Med.* <https://doi.org/10.1056/NEJMoa2105385> (2021).
- Greinacher, A. et al. Thrombotic thrombocytopenia after ChAdOx1 nCoV-19 vaccination. *N. Engl. J. Med.* <https://doi.org/10.1056/NEJMoa2104840> (2021).
- Schultz, N. H. et al. Thrombosis and thrombocytopenia after ChAdOx1 nCoV-19 vaccination. *N. Engl. J. Med.* <https://doi.org/10.1056/NEJMoa2104882> (2021).
- Sahin, U. et al. An RNA vaccine drives immunity in checkpoint-inhibitor-treated melanoma. *Nature* **585**, 107–112 (2020).
- Brahmer, J. R. et al. Phase I study of single-agent anti-programmed death-1 (MDX-1106) in refractory solid tumors: safety, clinical activity, pharmacodynamics, and immunologic correlates. *J. Clin. Oncol.* **28**, 3167–3175 (2010).
- Tumeh, P. C. et al. PD-1 blockade induces responses by inhibiting adaptive immune resistance. *Nature* **515**, 568–571 (2014).
- Farber, D. L., Yudanin, N. A. & Restifo, N. P. Human memory T cells: generation, compartmentalization and homeostasis. *Nat. Rev. Immunol.* **14**, 24–35 (2014).
- Johnson, D. B. et al. Fulminant myocarditis with combination immune checkpoint blockade. *N. Engl. J. Med.* **375**, 1749–1755 (2016).
- Ballhausen, A. et al. The shared frameshift mutation landscape of microsatellite-unstable cancers suggests immunoediting during tumor evolution. *Nat. Commun.* **11**, 4740 (2020).
- Postow, M. A., Sidlow, R. & Hellmann, M. D. Immune-related adverse events associated with immune checkpoint blockade. *N. Engl. J. Med.* **378**, 158–168 (2018).
- Monin, L. et al. Safety and immunogenicity of one versus two doses of the COVID-19 vaccine BNT162b2 for patients with cancer: interim analysis of a prospective observational study. *Lancet Oncol.* [https://doi.org/10.1016/S1470-2045\(21\)00213-8](https://doi.org/10.1016/S1470-2045(21)00213-8) (2021).
- Waissengrin, B. et al. Short-term safety of the BNT162b2 mRNA COVID-19 vaccine in patients with cancer treated with immune checkpoint inhibitors. *Lancet Oncol.* **22**, 581–583 (2021).
- Desai, A. et al. COVID-19 vaccine guidance for patients with cancer participating in oncology clinical trials. *Nat. Rev. Clin. Oncol.* **18**, 313–319 (2021).
- Williamson, E. J. et al. Factors associated with COVID-19-related death using OpenSAFELY. *Nature* **584**, 430–436 (2020).
- Deng, G. et al. Clinical determinants for fatality of 44,672 patients with COVID-19. *Crit. Care* **24**, 179 (2020).
- Ribas, A. et al. Priority COVID-19 vaccination for patients with cancer while vaccine supply is limited. *Cancer Discov.* **11**, 233–236 (2020).

Publisher's note Springer Nature remains neutral with regard to jurisdictional claims in published maps and institutional affiliations.



Open Access This article is licensed under a Creative Commons Attribution 4.0 International License, which permits use, sharing, adaptation, distribution and reproduction in any medium or format, as long as you give appropriate credit to the original author(s) and the source, provide a link to the Creative Commons license, and indicate if changes were made. The images or other third party material in this article are included in the article's Creative Commons license, unless indicated otherwise in a credit line to the material. If material is not included in the article's Creative Commons license and your intended use is not permitted by statutory regulation or exceeds the permitted use, you will need to obtain permission directly from the copyright holder. To view a copy of this license, visit <http://creativecommons.org/licenses/by/4.0/>.

© The Author(s) 2021

Crick COVID-19 Consortium

George Kassiotis⁸, Sonia Gandhi^{9,10} and Charles Swanton¹¹

A full list of members appears in the Supplementary Information.

CAPTURE Consortium

Lewis Au^{1,2}, Annika Fendler¹, Scott T. C. Shepherd^{1,2}, Fiona Byrne¹, Ben Shum^{1,2}, Camille Gerard^{1,6}, Kate Young², Lisa Pickering², Andrew J. S. Furness², James Larkin², George Kassiotis⁸, Katalin A. Wilkinson³, Robert J. Wilkinson^{3,4}, Susana Banerjee¹⁴, Naureen Starling¹³, Ian Chau¹³ and Samra Turajlic^{1,2}

A full list of members appears in the Supplementary Information.

Methods

CAPTURE design, study schedule and follow-up. During admission, the patient was enrolled in CAPTURE (NCT03226886; see Supplementary Material for a list of consortium members), an observational prospective study of the immune response to SARS-CoV-2 in patients with cancer that opened for recruitment in May 2020 at the Royal Marsden NHS Foundation Trust. The study design was previously published²⁵. Adult patients with current or history of invasive cancer are eligible for enrolment, irrespective of cancer type, stage or treatment. Primary and secondary endpoints relate to patient characteristics of those with and without SARS-CoV-2 infection and the effect of COVID-19 on long-term survival and intensive care unit admission rates. Exploratory endpoints pertain to characterizing clinical and immunological determinants of COVID-19 and vaccine response in patients with cancer. Clinical data and sample collection for participating patients with cancer are performed at baseline and at clinical visits per standard-of-care management during the first year of follow-up; frequency varies depending on inpatient or outpatient status and systemic anti-cancer treatment regimens. CAPTURE was approved as a substudy of TRACERx Renal (NCT03226886). TRACERx Renal was initially approved by the National Research Ethics Service (NRES) Committee London - Fulham on 17 January 2012. The TRACERx Renal sub-study CAPTURE was submitted as part of Substantial Amendment 9 and approved by the Health Research Authority on 30 April 2020 and the NRES Committee London - Fulham on 1 May 2020. The CAPTURE protocol was approved by institutional review boards and ethics committees, and the participant in this case report gave written informed consent for sample collection and use, according to CARE guidelines and in compliance with Declaration of Helsinki principles.

Adverse events grading. All adverse events were graded per Common Terminology Criteria for Adverse Events version 4.03.

Handling of whole blood samples. For indicated experiments, serum or plasma samples were heat inactivated at 56 °C for 30 min before use.

Plasma and peripheral blood mononuclear cell isolation. Whole blood was collected in EDTA tubes (VWR) and stored at 4 °C until processing. All samples were processed within 24 h. Time of blood draw, processing and freezing was recorded for each sample. Before processing, tubes were brought to room temperature. Peripheral blood mononuclear cells (PBMCs) and plasma were isolated by density gradient centrifugation using pre-filled centrifugation tubes (pluriSelect). Up to 30 ml of undiluted blood was added on top of the sponge and centrifuged for 30 min at 1,000g at room temperature. Plasma was carefully removed and then centrifuged for 10 min at 4,000g to remove debris, aliquoted and stored at -80 °C. The cell layer was then collected and washed twice in PBS by centrifugation for 10 min at 300g at room temperature. PBMCs were resuspended in Recovery Cell Culture Freezing Medium (Thermo Fisher Scientific) containing 10% DMSO, placed overnight in CoolCell freezing containers (Corning) at -80 °C and then stored in liquid nitrogen.

Serum isolation. Whole blood was collected in serum coagulation tubes (Vacuette CAT tubes, Greiner Bio-One) for serum isolation and stored at 4 °C until processing. All samples were processed within 24 h. Time of blood draw, processing and freezing was recorded for each sample. Tubes were centrifuged for 10 min at 2,000g at 4 °C. Serum was separated from the clotted portion, aliquoted and stored at -80 °C.

S1-reactive IgG ELISA. Ninety-six-well MaxiSorp plates (Thermo Fisher Scientific) were coated overnight at 4 °C with purified S1 protein in PBS (3 µg ml⁻¹ per well in 50 µl) and blocked for 1 h in blocking buffer (PBS, 5% milk, 0.05% Tween 20 and 0.01% sodium azide). Sera were diluted in blocking buffer (1:50). Fifty microliters of serum was then added to the wells and incubated for 2 h at room temperature. After washing four times with PBS-T (PBS and 0.05% Tween 20), plates were incubated with alkaline phosphatase-conjugated goat anti-human IgG (1:1,000, Jackson ImmunoResearch) for 1 h. Plates were developed by adding 50 µl of alkaline phosphatase substrate (Sigma-Aldrich) for 15–30 min after six washes with PBS-T. Optical densities were measured at 405 nm on a microplate reader (Tecan). CR3022 (Absolute Antibody) was used as a positive control. The cutoff for a positive response was defined as the mean negative value multiplied by 0.35 times the mean positive value.

Neutralizing antibody assay. Confluent monolayers of Vero E6 cells were incubated with SARS-CoV-2 virus and two-fold serial dilutions of heat-treated serum or plasma samples starting at 1:40 for 4 h at 37 °C in 5% CO₂ in duplicates. The inoculum was then removed, and cells were overlaid with viral growth medium. Cells were incubated at 37 °C in 5% CO₂. At 24 h after infection, cells were fixed in 4% paraformaldehyde (PFA) and permeabilized with 0.2% Triton X-100/PBS. Virus plaques were visualized by immunostaining, as described previously²⁶ for the neutralization of influenza viruses using a rabbit polyclonal anti-NSP8 antibody used at 1:1,000 dilution and anti-rabbit horseradish peroxidase (HRP)-conjugated antibody at 1:1,000 dilution and detected by action of HRP on

a tetramethyl benzidine-based substrate. Virus plaques were quantified, and ID₅₀ was calculated.

T cell stimulation. PBMCs for in vitro stimulation were thawed at 37 °C and resuspended in 10 ml of warm complete medium (RPMI and 5% human AB serum) containing 0.02% benzonase. Viable cells were counted, and 2 × 10⁶ cells were seeded in 200 µl of complete medium per well of a 96-well plate. Cells were stimulated with 4 µl per well of PepTivator SARS-CoV-2 S, M, or N pools (representing 1 µg ml⁻¹ final concentration per peptide; Miltenyi Biotec). Staphylococcal enterotoxin B (Merck) was used as a positive control at 0.5 µg ml⁻¹ final concentration; negative control was PBS containing DMSO at 0.002% final concentration. PBMCs were cultured for 24 h at 37 °C in 5% CO₂.

Activation-induced marker assay. Cells were washed twice in warm PBMCs. Dead cells were stained with 0.5 µl per well of Zombie dye V500 for 15 min at room temperature in the dark and then washed once with PBS containing 2% FCS (FACS buffer). A surface staining mix was prepared per well, containing 2 µl per well of each antibody for surface staining (Supplementary Table 1) in 50:50 brilliant stain buffer (BD Biosciences) and FACS buffer. PBMCs were stained with 50 µl of surface staining mix per well for 30 min at room temperature in the dark. Cells were washed once in FACS buffer and fixed in 1% PFA in FACS buffer for 20 min and then washed once and resuspended in 200 µl of PBS. All samples were acquired on a Bio-Rad ZE5 flow cytometer running Bio-Rad Everest software version 2.4 and analyzed using FlowJo version 10 (Tree Star) analysis software. Compensation was performed with 20 µl of antibody-stained Anti-Mouse Ig, κ/Negative Control Compensation Particles Set (BD Biosciences). Up to 1 × 10⁶ live CD19⁻CD14⁻ cells were acquired per sample. Gates were drawn relative to the unstimulated control for each donor. Gating strategy is shown in Supplementary Fig. 2c. T cell response is displayed as a stimulation index by dividing the percentage of apoptosis inhibitor of macrophage (AIM)-positive cells by the percentage of cells in the negative control. When S, M and N stimulation were combined, the sum of AIM-positive cells was divided by the three times the percentage of positive cells in the negative control.

ELISpot assay. IFN-γ pre-coated ELISpot plates (Mabtech) were blocked with complete medium (RPMI and 5% human AB serum) before 300,000 PBMCs were seeded per well and stimulated for 18 h with 2 µl per well of PepTivator SARS-CoV-2 S, M or N pools (representing 1 µg ml⁻¹ final concentration per peptide; Miltenyi Biotec). Plates were developed with human biotinylated IFN-γ detection antibody (7-B6-1-ALP, 1:200), followed by incubation with BCIP/NBT Phosphatase Substrate (SeraCare). Spot-forming units (SFU) were quantified with ImmunoSpot (Mabtech). To quantify positive peptide-specific responses, spots of the unstimulated wells were subtracted from the peptide-stimulated wells, and the results were expressed as SFU/106 PBMCs.

Multiplex immune assay for cytokines and chemokines. The pre-configured multiplex Human Immune Monitoring 65-plex ProcartaPlex immunoassay kit (Invitrogen, Thermo Fisher Scientific) was used to measure 65 protein targets in plasma on the Bio-Plex platform (Bio-Rad Laboratories), using Luminex xMAP technology. Analytes measured included APRIL; BAFF; BLC; CD30; CD40L; ENA-78; eotaxin; eotaxin-2; eotaxin-3; FGF-2; fractalkine; G-CSF; GM-CSF; GRO-alpha; HGF; IFN-α; IFN-γ; IL-10; IL-12p70; IL-13; IL-15; IL-16; IL-17A; IL-18; IL-1α; IL-1β; IL-2; IL-20; IL-21; IL-22; IL-23; IL-27; IL-2R; IL-3; IL-31; IL-4; IL-5; IL-6; IL-7; IL-8; IL-9; IP-10; I-TAC; LIF; MCP-1; MCP-2; MCP-3; M-CSF; MDC; MIF; MIG; MIP-1β; MIP-1α; MIP-3α; MMP-1; NGF-β; SCF; SDF-1α; TNF-β; TNF-α; TNF-R2; TRAIL; TSLP; TWEAK; and VEGF-A. All assays were conducted as per manufacturer recommendations.

SERA. Patient serum samples were screened and analyzed using the previously published SERA pipeline²⁷. Briefly, sera were screened with a randomized bacterial peptide display library, and plasmids from antibody-bound bacteria were isolated and sequenced. PIWAS was applied to identify epitopes and antigens for the SARS-CoV-2 proteome.

PF-4 IgG assay. Patient serum samples were analyzed using the LIFECODES PF-4 IgG Solid Phase ELISA microwells assay (Immucor). Briefly, diluted serum and controls were added to microwells coated with PF-4 complexed to polyvinyl sulfonate, incubated for 45 min at 37 °C and washed. IgG conjugate was added and incubated for 45 min at 37 °C. Plates were developed by incubation PNPP solution. Absorbance of each well was read at 405 nm. A positive and negative serum control was measured on the same plate. Values greater than 0.4 were considered positive.

Reporting Summary. Further information on research design is available in the Nature Research Reporting Summary linked to this article.

Data availability

All requests for raw and analyzed data, materials and CAPTURE study protocol will be reviewed by the CAPTURE Trials Team, Skin and Renal Clinical Trials Unit, The Royal Marsden NHS Foundation Trust (CAPTURE@rmh.nhs.uk) to

determine whether the request is subject to confidentiality and data protection obligations. Data and materials that can be shared will be released via a material transfer agreement.

References

- Au, L. et al. Cancer, COVID-19, and antiviral Immunity: the CAPTURE study. *Cell* **183**, 4–10 (2020).
- Wrobel, A. G. et al. Antibody-mediated disruption of the SARS-CoV-2 spike glycoprotein. *Nat. Commun.* **11**, 5337 (2020).
- Reifert, J. et al. Serum epitope repertoire analysis enables early detection of Lyme disease with improved sensitivity in an expandable multiplex format. *J. Clin. Microbiol.* **59**, e01836–20 (2021).

Acknowledgements

We thank the patient for permission to report his case. We thank the CAPTURE trial team, including H. Ahmod, N. Ash, R. Dhaliwal, L. Dowdie, T. Foley, L. Holt, J. Korteweg, C. Lewis, K. Lingard, M. Mangwende, A. Murra, K. Peat, S. Sarker, N. Shaikh and F. Williams. We thank F. Gronthoud, G. Gardner, R. Shea and their teams for support on sample collation. We acknowledge the tremendous support from the clinical and research teams at participating units at the Royal Marsden Hospital, as well as A. Macklin-Doherty for consenting the patient. We thank M. Gavrielides for informatics support and B. Stockinger for valuable discussions. We also thank the Volunteer Staff at the Francis Crick Institute and the Crick COVID-19 Consortium (see Supplementary Material for a list of consortium members). Owing to limitations on cited references and the pace at which the field is evolving, we acknowledge researchers in COVID-19 vaccines and immune responses in patients with cancer. The CAPTURE study is a sub-study of TRACERx Renal and is sponsored by the Royal Marsden NHS Foundation Trust and funded from a grant from the Royal Marsden Cancer Charity Programme (ref. no. RMCC32). TRACERx Renal is partly funded by the National Institute for Health Research Biomedical Research Centre at the Royal Marsden Hospital and the Institute of Cancer Research (A109). This work was supported by the Francis Crick Institute, which receives its core funding from Cancer Research UK (FC010110, FC0010988, FC001218, FC001030, FC0010988, FC001218, FC001030, FC001099, FC001002 and FC001169) and the Wellcome Trust (FC010110, FC0010988, FC001218, FC001030, FC001099, FC001002 and FC001169). For the purpose of open access, the author has applied for a CC BY public copyright license to any Author Accepted Manuscript version arising from this submission.

Author contributions

S.T., L.A., S.S. and A.F. contributed to study design. L.A., K.R., A.F. and S.T. drafted the manuscript. S.S., A.F. and L.A. contributed to the collection and processing of clinical specimens. A.F., K.W. and M.C. performed laboratory analysis. A.F., L.A. and K.R. contributed to visualizations. S.S., L.A., N.J.-H., D.L., I.C., N.S. and C.F. provided clinical data. All authors critically reviewed the manuscript for intellectual content, approved the final version of the manuscript for submission and agreed to be accountable for all aspects of the work

Competing interests

L.A. is funded by the Royal Marsden Cancer Charity. A.F. has received funding from the European Union's Horizon 2020 Research and Innovation Programme under Marie Skłodowska-Curie grant agreement no. 892360. M.C., K.A.W. and R.J.W. receive core funding from the Francis Crick Institute (FC001218). J.S. and W.H. are employees and shareholders at Serimmune. N.J.-H. receives funding from Cancer Research UK (grant ref. no. C65320/A26413). J.L. has worked in a consulting or advisory role for Achilles Therapeutics, AstraZeneca, Boston Biomedical, Bristol Myers Squibb, Eisai, EUSA Pharma, GlaxoSmithKline, Imugene, Incyte, iOnctura, Ipsen, Kymab, Merck Serono, Merck Sharp & Dohme, Nektar Therapeutics, Novartis, Pierre Fabre, Pfizer, Roche/Genentech, Secarna and Vitaccess and has received support from NIHR RM/ICR Biomedical Research Centre for Cancer and institutional research support from Achilles Therapeutics, Aveo, Bristol Myers Squibb, Covance, Immunocore, Merck Sharp & Dohme, Nektar Therapeutics, Novartis, Pharmacyclics, Pfizer and Roche. C.S. acknowledges grant support from Pfizer, AstraZeneca, Bristol Myers Squibb, Roche-Ventana, Boehringer Ingelheim, Archer Dx (collaboration in minimal residual disease sequencing technologies) and Ono Pharmaceutical. C.S. is an AstraZeneca Advisory Board member and Chief Investigator for the MeRmaiD1 clinical trial.

C.S. has consulted for Amgen, AstraZeneca, Bicycle Therapeutics, Bristol Myers Squibb, Celgene, Genentech, GlaxoSmithKline, GRAIL, Illumina, Medixci, Merck Sharp & Dohme, Novartis, Pfizer, Roche-Ventana and the Sarah Cannon Research Institute. C.S. has stock options in Apogen Biotechnologies, Epic Biosciences and GRAIL and has stock options and is co-founder of Achilles Therapeutics. C.S. holds pending patents relating to assay technology to detect tumor recurrence (PCT/GB2017/053289); targeting neoantigens (PCT/EP2016/059401); identifying patent response to immune checkpoint blockade (PCT/EP2016/071471); determining whether HLA LOH is lost in a tumor (PCT/GB2018/052004); predicting survival rates of patients with cancer (PCT/GB2020/050221); treating cancer by targeting insertion/deletion mutations (PCT/GB2018/051893); identifying insertion/deletion mutation targets (PCT/GB2018/051892); methods for lung cancer detection (PCT/US2017/028013); and identifying responders to cancer treatment (PCT/GB2018/051912). C.S. is Royal Society Napier Research Professor (RP150154). His work is supported by the Francis Crick Institute, which receives its core funding from Cancer Research UK (FC001169), the UK Medical Research Council (FC001169) and the Wellcome Trust (FC001169). C.S. is funded by Cancer Research UK (TRACERx, PEACE and CRUK Cancer Immunotherapy Catalyst Network), Cancer Research UK Lung Cancer Centre of Excellence (C11496/A30025), the Rosetrees Trust, the Butterfield and Stonegate Trusts, NovoNordisk Foundation (ID16584), a Royal Society Professorship Enhancement Award (RP/EA/180007), the National Institute for Health Research (NIHR) Biomedical Research Centre at University College London Hospitals, the Cancer Research UK-University College London Centre, the Experimental Cancer Medicine Centre, the Breast Cancer Research Foundation (BCRF) and a Stand Up To Cancer-LUNGevity-American Lung Association Lung Cancer Interception Dream Team Translational Research Grant (SU2C-AACR-DT23-17). Stand Up To Cancer is a program of the Entertainment Industry Foundation. Research grants are administered by the American Association for Cancer Research, the Scientific Partner of SU2C. C.S. receives funding from the European Research Council (ERC) under the European Union's Seventh Framework Programme (FP7/2007-2013) Consolidator Grant (FP7-THESEUS-617844), European Commission ITN (FP7-PloidyNet 607722), an ERC Advanced Grant (PROTEUS) from the European Research Council under the European Union's Horizon 2020 research and innovation programme (grant agreement 835297) and Chromavision from the European Union's Horizon 2020 research and innovation programme (grant agreement 665233). D.L. is the recipient of the Australasian Gastro-Intestinal Trials Group/Merck Clinical Research Fellowship. S.B. has worked in an advisory role for Amgen, AstraZeneca, Clovis Oncology, Epsilogen, Genmab, GlaxoSmithKline, Immunogen, Mersana, Merck Sharp & Dohme, Merck Sereno, Oncxerna, Pfizer, Tesaro and Roche; has received institution research funding from AstraZeneca; and has received funding support from NIHR RM/ICR Biomedical Research Centre for Cancer. I.C. has worked in a consulting or advisory role for Eli Lilly, Bristol Myers Squibb, Merck Sharp & Dohme, Bayer, Roche, Merck Serono, Five Prime Therapeutics, AstraZeneca, OncXerna, Pierre Fabre, Boehringer Ingelheim, Incyte and Astellas; has received research funding from Eli Lilly and Janssen-Cilag; and has received honoraria from Eli Lilly and Eisai. S.T. has received speaking fees from Roche, AstraZeneca, Novartis and Ipsen. G.K. receives core funding from the Francis Crick Institute (FC0010099). S.T. is funded by Cancer Research UK (grant ref. no. C50947/A18176), the Francis Crick Institute (which receives its core funding from Cancer Research UK (FC0010988)), the UK Medical Research Council (FC0010988) and the Wellcome Trust (FC0010988)), the National Institute for Health Research Biomedical Research Centre at the Royal Marsden Hospital and the Institute of Cancer Research (grant ref. no. A109), the Royal Marsden Cancer Charity, the Rosetrees Trust (grant ref. no. A2204), Ventana Medical Systems (grant ref. nos. 10467 and 10530), the National Institutes of Health and the Melanoma Research Alliance. All other authors declare no financial conflicts of interest.

Additional information

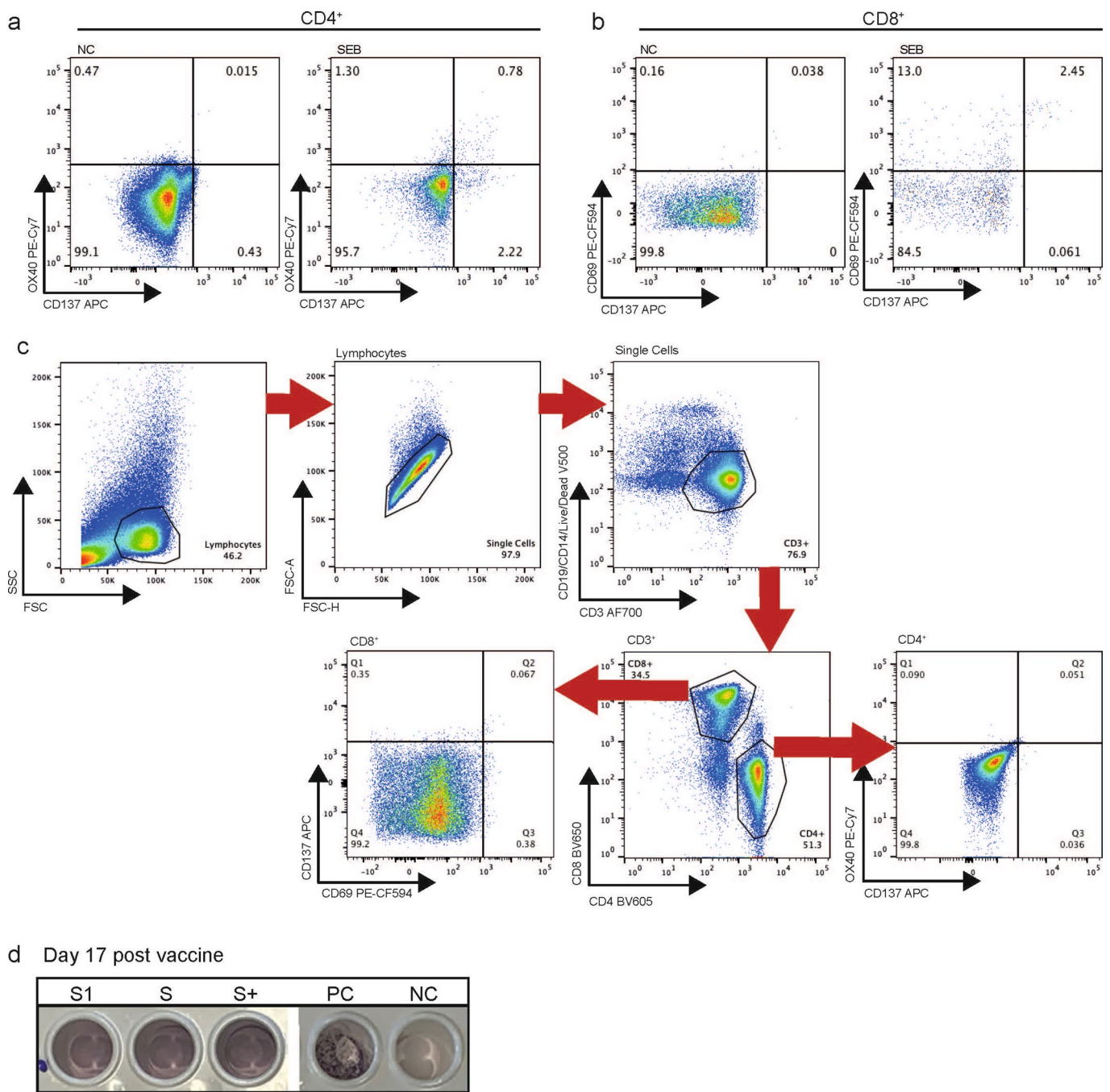
Extended data is available for this paper at <https://doi.org/10.1038/s41591-021-01387-6>.

Supplementary information The online version contains supplementary material available at <https://doi.org/10.1038/s41591-021-01387-6>.

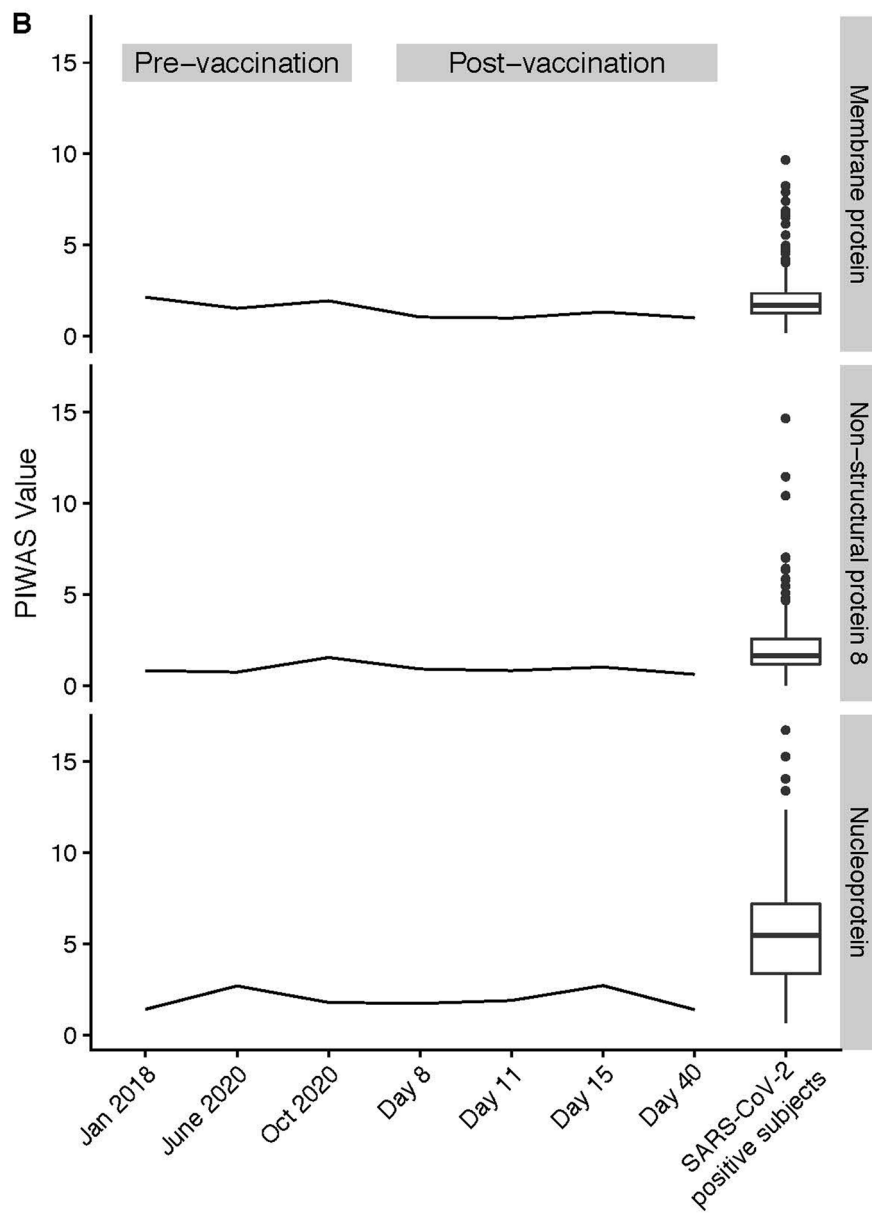
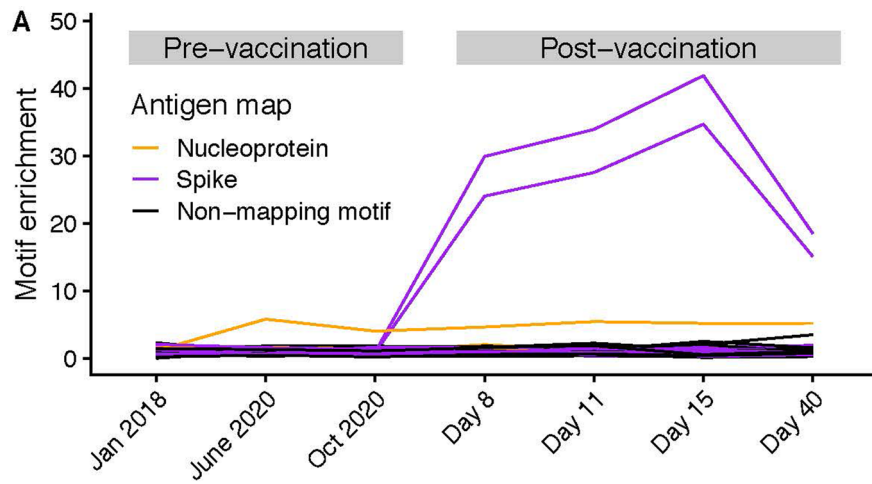
Correspondence and requests for materials should be addressed to S.T.

Peer review information *Nature Medicine* thanks Matthew Galsky and the other, anonymous, reviewer(s) for their contribution to the peer review of this work. Saheli Sadanand was the primary editor on this article and managed its editorial process and peer review in collaboration with the rest of the editorial team.

Reprints and permissions information is available at www.nature.com/reprints.

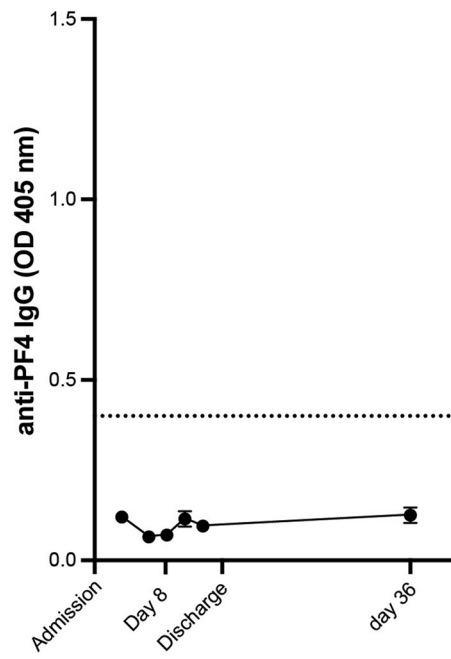


Extended Data Fig. 1 | Gating strategy for T-cell assay. a, CD4⁺ T-cell response to SEB in exemplary samples. **b**, CD8⁺ T-cell response to SEB in exemplary samples. **c**, Gating strategy for flow analysis of T-cell activation. PBMCs were stimulated with SEB for 24 hrs. SEB, Staphylococcal enterotoxin B. **d**, IFN- γ ELISpot at day 17 post vaccine. PBMCs were stimulated with S, S1 and S+ peptide pools representing the full length of the spike protein. Anti-CD3 antibody was used as a positive control (PC), no stimulation was added to the negative control (NC).



Extended Data Fig. 2 | See next page for caption.

Extended Data Fig. 2 | Antibody response to BNT162b2 according to SERA and PIWAS. **a**, Pre- and post-vaccination antibody levels against SARS-CoV-2 antigenic motifs. **b**, PIWAS values pre- and post-vaccination against non-spike sequences of the SARS-CoV-proteome compared to patients with SARS-CoV-2 positive subjects²⁴ (Methods). Box plots of PIWAS values of SARS-CoV-2 positive subjects are shown, where boxes denote the IQR, and the median is shown as horizontal bars. Whiskers extend to 1.5x IQR and outliers are shown as individual points (n = 230 subjects; n = 230 biologically independent samples). IQR, interquartile range; PIWAS, protein-based immunome wide association study; SERA, serum epitope repertoire analysis.



Extended Data Fig. 3 | Anti-PF4 antibodies after vaccination. Serum samples collected after admission were analysed for presence of anti-PF4 antibodies by ELISA. Values represent mean of two technical replicates, error bars represent standard deviation. The dotted line indicates the threshold for a sample to be considered positive (OD 450 nm > 0.4).

Reporting Summary

Nature Research wishes to improve the reproducibility of the work that we publish. This form provides structure for consistency and transparency in reporting. For further information on Nature Research policies, see our [Editorial Policies](#) and the [Editorial Policy Checklist](#).

Statistics

For all statistical analyses, confirm that the following items are present in the figure legend, table legend, main text, or Methods section.

n/a Confirmed

- The exact sample size (n) for each experimental group/condition, given as a discrete number and unit of measurement
- A statement on whether measurements were taken from distinct samples or whether the same sample was measured repeatedly
- The statistical test(s) used AND whether they are one- or two-sided
Only common tests should be described solely by name; describe more complex techniques in the Methods section.
- A description of all covariates tested
- A description of any assumptions or corrections, such as tests of normality and adjustment for multiple comparisons
- A full description of the statistical parameters including central tendency (e.g. means) or other basic estimates (e.g. regression coefficient) AND variation (e.g. standard deviation) or associated estimates of uncertainty (e.g. confidence intervals)
- For null hypothesis testing, the test statistic (e.g. F , t , r) with confidence intervals, effect sizes, degrees of freedom and P value noted
Give P values as exact values whenever suitable.
- For Bayesian analysis, information on the choice of priors and Markov chain Monte Carlo settings
- For hierarchical and complex designs, identification of the appropriate level for tests and full reporting of outcomes
- Estimates of effect sizes (e.g. Cohen's d , Pearson's r), indicating how they were calculated

Our web collection on [statistics for biologists](#) contains articles on many of the points above.

Software and code

Policy information about [availability of computer code](#)

Data collection

Data analysis

For manuscripts utilizing custom algorithms or software that are central to the research but not yet described in published literature, software must be made available to editors and reviewers. We strongly encourage code deposition in a community repository (e.g. GitHub). See the Nature Research [guidelines for submitting code & software](#) for further information.

Data

Policy information about [availability of data](#)

All manuscripts must include a [data availability statement](#). This statement should provide the following information, where applicable:

- Accession codes, unique identifiers, or web links for publicly available datasets
- A list of figures that have associated raw data
- A description of any restrictions on data availability

All requests for raw and analysed data, materials, and CAPTURE study protocol will be reviewed by the CAPTURE Trials Team, Skin and Renal Clinical Trials Unit, The Royal Marsden NHS Foundation Trust (CAPTURE@rmh.nhs.uk) to determine if the request is subject to confidentiality and data protection obligations. Data and materials that can be shared will be released via a material transfer agreement.

Field-specific reporting

Please select the one below that is the best fit for your research. If you are not sure, read the appropriate sections before making your selection.

Life sciences Behavioural & social sciences Ecological, evolutionary & environmental sciences

For a reference copy of the document with all sections, see [nature.com/documents/nr-reporting-summary-flat.pdf](https://www.nature.com/documents/nr-reporting-summary-flat.pdf)

Life sciences study design

All studies must disclose on these points even when the disclosure is negative.

Sample size	<input type="text" value="This is a case report (n=1)."/>
Data exclusions	<input type="text" value="No data were excluded."/>
Replication	<input type="text" value="For correlative measures, all human specimens underwent quality control (QC) assessments. Only those that passed QC were further analyzed"/>
Randomization	<input type="text" value="This is a case report (n=1)."/>
Blinding	<input type="text" value="This is a case report and thus blinding was not performed."/>

Reporting for specific materials, systems and methods

We require information from authors about some types of materials, experimental systems and methods used in many studies. Here, indicate whether each material, system or method listed is relevant to your study. If you are not sure if a list item applies to your research, read the appropriate section before selecting a response.

Materials & experimental systems

Methods

n/a	Involvement in the study	n/a	Involvement in the study
<input type="checkbox"/>	<input checked="" type="checkbox"/> Antibodies	<input checked="" type="checkbox"/>	<input type="checkbox"/> ChIP-seq
<input checked="" type="checkbox"/>	<input type="checkbox"/> Eukaryotic cell lines	<input type="checkbox"/>	<input checked="" type="checkbox"/> Flow cytometry
<input checked="" type="checkbox"/>	<input type="checkbox"/> Palaeontology and archaeology	<input checked="" type="checkbox"/>	<input type="checkbox"/> MRI-based neuroimaging
<input checked="" type="checkbox"/>	<input type="checkbox"/> Animals and other organisms		
<input type="checkbox"/>	<input checked="" type="checkbox"/> Human research participants		
<input type="checkbox"/>	<input checked="" type="checkbox"/> Clinical data		
<input checked="" type="checkbox"/>	<input type="checkbox"/> Dual use research of concern		

Antibodies

Antibodies used	<input type="text" value="A list of antibodies is provided in Table S1"/>
Validation	<input type="text" value="Antibodies for AIM assay were chosen on the basis of previous publication of the assay (Grifoni et al. Targets of T Cell Responses to SARS-CoV-2 Coronavirus in Humans with COVID-19 Disease and Unexposed Individuals. Cell.) References with validation of other primary antibodies used are as follows: Neutralising antibodies (NSP8 and anti-rabbit IgG - Wrobel et al. Antibody-mediated disruption of the SARS-CoV-2 spike glycoprotein. Nat Comm.; ELISpot assay antibodies (https://www.mabtech.com/products/human-ifn-gamma-elisa-pro-kit_3420-1hp-10)."/>

Human research participants

Policy information about [studies involving human research participants](#)

Population characteristics	<input type="text" value="Single human subject. 58 year old male with history of metastatic mismatch repair deficient colorectal cancer on anti-PD1 monotherapy."/>
Recruitment	<input type="text" value="CAPTURE study (NCT03226886)"/>
Ethics oversight	<input type="text" value="CAPTURE was approved as a substudy of TRACERx Renal (NCT03226886). TRACERx Renal was initially approved by the NRES Committee London - Fulham on January 17, 2012. The TRACERx Renal sub-study CAPTURE was submitted as part of Substantial Amendment 9 and approved by the Health Research Authority on April 30, 2020 and the NRES Committee London - Fulham on May 1, 2020. CAPTURE is conducted in accordance with the ethical principles of the Declaration of Helsinki, Good Clinical Practice and applicable regulatory requirements."/>

Clinical data

Policy information about [clinical studies](#)

All manuscripts should comply with the ICMJE [guidelines for publication of clinical research](#) and a completed [CONSORT checklist](#) must be included with all submissions.

Clinical trial registration	CAPTURE study (NCT03226886)
Study protocol	Request for protocols should be directed to CAPTURE trials unit via CAPTURE@rmh.nhs.uk
Data collection	Data was collected at Royal Marsden hospital, by extract from clinical records approved as per protocol. The participant was recruited on the 13/1/21.
Outcomes	Vaccine efficacy, immunological parameters, and associations with clinical features presented are exploratory endpoints of this study. Primary endpoint of study is description of population characteristics between SARS-CoV-2 positive and negative cancer patients. Secondary endpoints are differences in overall survival, intensive treatment unit admission rate, anti-cancer treatment received, and immune related adverse events.

Flow Cytometry

Plots

Confirm that:

- The axis labels state the marker and fluorochrome used (e.g. CD4-FITC).
- The axis scales are clearly visible. Include numbers along axes only for bottom left plot of group (a 'group' is an analysis of identical markers).
- All plots are contour plots with outliers or pseudocolor plots.
- A numerical value for number of cells or percentage (with statistics) is provided.

Methodology

Sample preparation	Whole blood was collected in EDTA tubes (VWR) and stored at 4°C until processing. All samples were processed within 24 hours. Time of blood draw, processing, and freezing was recorded for each sample. Prior to processing tubes were brought to room temperature (RT). PBMC and plasma were isolated by density-gradient centrifugation using pre-filled centrifugation tubes (pluriSelect). Up to 30 ml of undiluted blood was added on top of the sponge and centrifuged for 30 minutes at 1000 x g at RT. Plasma was carefully removed then centrifuged for 10 minutes at 4000 x g to remove debris, aliquoted and stored at -80°C. The cell layer was then collected and washed twice in PBS by centrifugation for 10 minutes at 300 x g at RT. PBMC were resuspended in Recovery cell culture freezing medium (Fisher Scientific) containing 10% DMSO.
Instrument	All experiments were run on a Bio-Rad Ze5 flow cytometer running Bio-Rad Everest software v2.4
Software	Data were analysed using FlowJo 10.7.1
Cell population abundance	Cells were not sorted in this study
Gating strategy	Lymphocytes were gated in FSC-A/SSC-A plot, followed by gating for singlets by plotting FSC-A vs. FSC-H. Viable CD3+ cells were identified by plotting CD3 vs. CD14, CD19, and viability dye. Next CD4+ and CD4+ cells were gated and finally CD137+OX40+ cells were identified in the CD4+ population and CD137+CD69+ in the CD8+ population.

- Tick this box to confirm that a figure exemplifying the gating strategy is provided in the Supplementary Information.